Available online at www.sciencedirect.com

ScienceDirect

IFAC PapersOnline CONFERENCE PAPER ARCHIVE

IFAC PapersOnLine 58-28 (2024) 750–755

Real time camera-based sideslip angle estimation: design and experiments

Leonardo Serena * **Mattia Bruschetta** ** **Giovanni Righetti** ***
Ricardo de Castro **** **Basilio Lenzo** †

* *University of Padova, Padova, Italy (e-mail: leonardo.serena@unipd.it).*
** *University of Padova, Padova, Italy (e-mail: mattia.bruschetta@unipd.it).*
*** *University of Padova, Padova, Italy (e-mail: giovanni.righetti.3@phd.unipd.it).*
**** *University of California at Merced, Merced, CA 95343 USA (e-mail: rpintodecastro@ucmerced.edu).*
† *University of Padova, Padova, Italy (e-mail: basilio.lenzo@unipd.it).*

Abstract: Vehicle stability controllers and car modeling significantly rely on the knowledge of the vehicle velocity and sideslip angle, i.e. the angle between the velocity vector and the vehicle's heading. While various estimation techniques have been proposed over time, their reliability across generic driving scenarios remains unsatisfactory. This study investigates a novel methodology to directly measure velocity and sideslip angle, using computer vision techniques. A real-time sensing framework is put in place on a full-scale passenger vehicle, with the camera setup allowing to send signals over the vehicle Controller Area Network (CAN). Experiments, along several manoeuvres, confirm the real-time applicability and effectiveness of the proposed approach against the state-of-the-art sensor Kistler S-Motion (ground truth).

Keywords: Vehicle dynamics, sideslip angle, vehicle state estimation, computer vision.

1. INTRODUCTION

One of the main focuses of the automotive industry is the development of technologies designed to improve vehicle safety. For example, Advanced driver assistance systems (ADAS) include a variety of systems that enhance safety and improve the driving experience by automating, adapting, or enhancing vehicle systems. In order to obtain optimal performance and, most importantly, maximum safety, these systems require accurate knowledge of vehicle states. Many critical states of the vehicle are not practically measurable in a passenger vehicle, e.g. tire forces, tire slip, lateral velocity. The accurate knowledge of these states could greatly improve the effectiveness of ADAS.

Among key vehicle states, vehicle sideslip angle, β, plays a crucial role in vehicle stability. β is defined as the angle between the velocity of the vehicle centre of mass and the vehicle heading Guiggiani (2014). The knowledge of sideslip angle, which is related to vehicle lateral velocity, could be game-changing in the development of systems like electronic stability controllers (ESC) Hsu et al. (2009); Lenzo (2022). Actually β may be directly measured, but the cost of dedicated optical sensors prevents their use in commercial vehicles. Therefore plenty of research efforts have been devoted to the development of methods to estimate sideslip angle. By exploiting all the sensors already available in the vehicle, model based methods and data driven methods have been used to fuse all the information and obtain a reliable estimate of the sideslip angle Viehweger et al. (2021).

Model based solutions exploit vehicle models and measurements from standard on-board sensors, such as inertial measurement unit (IMU), to estimate the sideslip angle. The problem of model based solutions is their dependency on an accurate vehicle model. In fact, while simpler models are easily implemented and guarantee a low computational effort, they lack accuracy in the nonlinear working range of tires. On the other hand, complex nonlinear models are more accurate, but need more computational effort and their tuning is rather difficult. This also prompted recent efforts on adaptive models. For instance in Mosconi et al. (2022) an Extended Kalman filter (EKF) has been employed to estimate sideslip angle, modelling tires with a Pacejka's Magic Formula and with cornering stiffness values adapted online. In Katriniok and Abel (2016) the vehicle state includes two extra adaptation parameters, describing the longitudinal and lateral force variation on the tires, while a global navigation satellite system (GNSS) is exploited as another source of information in an EKF framework. A combination of a kinematic vehicle model and a dynamic vehicle model is used in Xia et al. (2023) in a consensus Kalman filter (CKF) framework to obtain the sideslip angle even with varying driving style. In light of the critical importance of a reliable vehicle model, data-based methods are also being explored based on the idea that artificial neural networks can overcome the issue of requiring high computational resources and detailed models.

10.1016/j.ifacol.2025.01.056

For instance in De Martino et al. (2017) a properly trained neural network has been employed to estimate sideslip angle with the onboard sensors of the vehicle, investigating the states that have the most impact in the computation of β. However, data-based methods require high amount of data and computational effort during the training process, and a further major weakness is their unsuitability in case of important changes of the system with respect to the training data.

A direct, low-cost way to measure sideslip angle would be the ideal solution, able to offer a consistent measurement in a wide variety of driving and environmental conditions (high and low friction, rain, snow, tire wear etc.). This is actually possible by employing a camera and image correlation techniques. Cameras have always been a crucial source of information in the aerospace sector, especially in rover development, as they can provide information about the position of the vehicle without resorting to sensors that are unreliable or unavailable in space. For instance Kazik and Goktogan (2011) applied a phase correlation (PC) technique to obtain the rover trajectory, from footage recorder with a down-facing camera. A similar set-up has been tested in a controlled setting in Birem et al. (2018). In Botha and Els (2014) the authors used a camera pointing to the tyre to compute longitudinal slip ratio by comparing the displacement of the tyre with respect to the road. Using the same correlation technique Botha and Els (2015) used a high-performance camera pointed at the road surface, to compute the velocity vector of the vehicle by comparing subsequent frames of the footage with the Lucas-Kanade optical flow algorithm. The same solution was implemented in a real time framework in Johnson et al. (2019). In Kuyt and Como (2018) a scaled radio controlled (RC) vehicle was used to obtain sideslip angle through a front facing camera and markers in the asphalt. Recently, in Serena et al. (2023) we investigated the effectiveness of different algorithms for camera-based sideslip angle measurement, endorsing the use of the phase correlation method.

In this paper, we propose a full methodology for the development of a camera-based velocity sensor, addressing important practical challenges such as roll-angle effects and real-time operability. Experiments are first conducted on a purposely-modified RC vehicle, to test the real time capability of the solution. Further experiments are then performed on a full-scale vehicle prototype on a proving ground, allowing a real-time comparison of the proposed methodology with a state-of-the-art commercial optical sensor.

The remainder of this paper is structured as follows. The motion estimation algorithm is described in Sec. 2. The proposed solution setup is described in Sec. 3, together with the testing vehicles. The real time capabilities of the solution are addressed in Sec. 4 and the results of the tests are discussed in Sec. 5, before concluding remarks in Sec. 6.

2. MOTION ESTIMATION

The determination of vehicle velocity can be achieved through the computation of camera optical flow, denoting the apparent motion of a stream of images during camera movement. Our proposed approach exploits the entirety of image pixels while maintaining a computationally manageable overhead. The idea is based on the shift property inherent in the Fourier transform for the computation of the spatial displacement between two images. The shifting property of the Fourier transform states that a temporal shift corresponds to a phase shift in the frequency domain. In the context of images, which can be seen as signals with information encoded in pixel positions rather than a temporal sequence, the assessment of the phase shift between two subsequent images corresponds to the assessment of their spatial displacement Birem et al. (2018). Therefore, given two subsequent pictures of the same subject, it is possible to obtain the spatial displacement in pixel quantities δ_x, δ_y. Assuming the camera to be pointing downwards with its z-axis perpendicular to the ground, the longitudinal and lateral velocity of the vehicle may be computed by knowing the camera height h, its focal distance in pixel f, and its frequency of acquisition ν.

Actually, having multiple pictures of the same object from different points of view, and knowing the camera characteristics, it is possible to map points in the 3D world to the 2D pixel coordinates and viceversa. A simple explanation of this can be obtained by employing the camera pinhole model Beaver (2018). In this context a point P defined by (X, Y, Z) in space is projected into the image plane into a 2D point $C = (X_p, Y_p)$. The point C depends on P and on the camera focal length, i.e. the distance between focal point and image plane. The map can be described by:

$$\left(f\frac{X}{Z}, f\frac{Y}{Z}\right) \longrightarrow (X, Y, Z) \tag{1}$$

The advantage of placing the camera perpendicular to the ground allows to assume $Z = h$ for all points of the image, therefore it is possible to associate a velocity vector to each pixel displacement by means of a simple proportion:

$$v_{x,y} = -\delta_{x,y} \cdot \frac{h}{f} \cdot \nu \tag{2}$$

where $v_{x,y}$ corresponds to the longitudinal or lateral velocity of the vehicle. It is clear that $v_{x,y}$ directly depends on the height of the camera h.

3. ARCHITECTURE

The camera-based system consists of an high speed camera and an image processing unit. The herein proposed solution employs a Basler Ace acA720-290gm as high speed camera, which is capable of shooting up to 291 fps (capped at 200 fps) and an Intel NUC 12 with Intel i7 processor as image processing unit.

Tests have been carried out on a radio-controlled (RC) vehicle and on a full-scale vehicle. The RC vehicle sessions allowed preliminary testing including system tuning and evaluation of the execution time. Such a set-up allows to drastically reduce costs and development time. The test session on the real vehicle also allowed to assess the accuracy of the measurement provided by the proposed camera-based solution, because our measurements were real-time compared with the measurements provided by the dedicated Kistler S-Motion optical sensor.

Radio Controlled vehicle The RC vehicle is a customized version of the Traxxas's Ledge 1:8 model. For this purpose

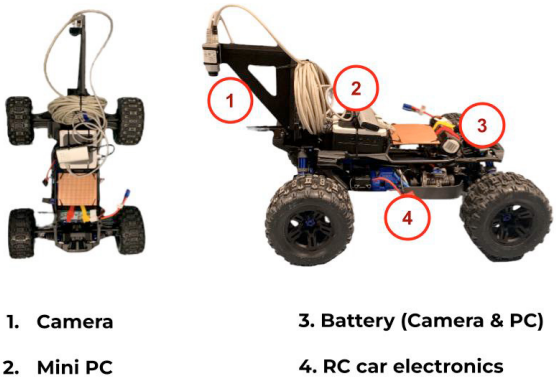

Fig. 1. Radio controlled vehicle system setup

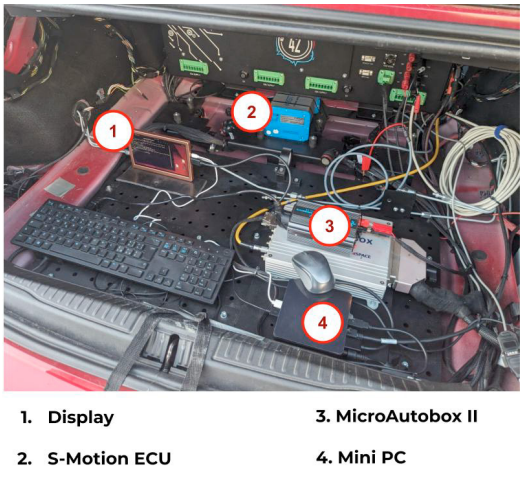

Fig. 2. Alfa Romeo Giulia system setup

we equipped it with an extra dedicated battery for the Intel NUC computer and the camera, as in Fig. 1. The processing unit is responsible for logging the computed absolute velocity and the time needed to complete each cycle.

Alfa Romeo Giulia The camera-based system is capable of interfacing directly with the data-logging platform - dSPace MicroAutobox II, see Fig. 2 - via dedicated CAN network. The logger samples all the measurements at 100 Hz. The first mounting location for the camera was on the vehicle side, specifically under the side mirror (location 1). The region of interest (ROI) acquired by the camera is configured to capture the highest amount of details (i.e. the asphalt) while minimizing the inclusion of parts of the car body which do not provide useful information. Still, such camera positioning is heavily affected by the roll angle of the vehicle, which changes the height of the camera from the ground. For this reason, a second mounting location was tried out in a second set of tests, positioning the camera at the rear of the vehicle (location 2). The maximum measurable velocity is lower as the ROI of location 2 is smaller than for location 1. The two locations are shown in Fig. 3.The height of the camera from the ground is $h_0 = 75$ cm for location 1, and $h = 98$ cm for location 2.

Practically, the alignment of the camera may not perfectly correspond to an ideal configuration, i.e. perpendicular

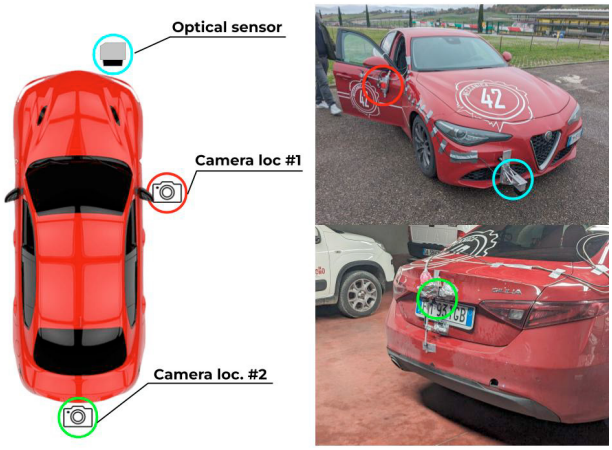

Fig. 3. Positions of the camera and of the optical sensor

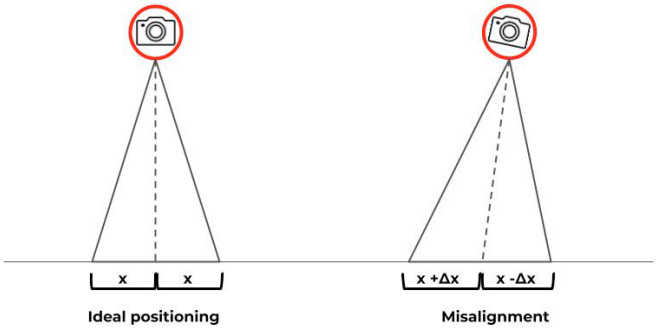

Fig. 4. Effect of the mounting angle of the camera

to the ground and aligned with the longitudinal axis of the vehicle (x). These inaccuracies lead to inherent measurement offsets, that are to be accounted for. An angular offset of the camera along the z-axis causes a constant offset in the sideslip angle. Rotations along the x and y axes undermine the assumption of perpendicularity, critical for the absolute velocity computation as in Eq. (2). Specifically, a misalignment on the x-axis may induce a lateral velocity offset (Fig. 4). This particular offset is quite challenging when it comes to correcting it, as it exhibits a proportionality to the velocity itself.

4. REAL TIME VALIDATION

The advantages of the proposed solutions are not only associated to the accuracy of the measurements, but also to its manageable computational burden. In fact, for each image comparison, the algorithm performs two Fast Fourier transforms, a matrix multiplication and find the maximum value in a matrix, see Serena et al. (2023). All these operations have bounded cost and depend directly on the resolution of the images: the more the pixels, the higher the execution time (T_c).

Figure 5 shows a generic test performed with the RC vehicle. The execution time is always below the 5 ms threshold T_c^{max}, which is the sampling time of the camera. This way the algorithm is capable of returning a velocity value before a new image is acquired. It should however be noted that the proposed algorithm is bounded in the

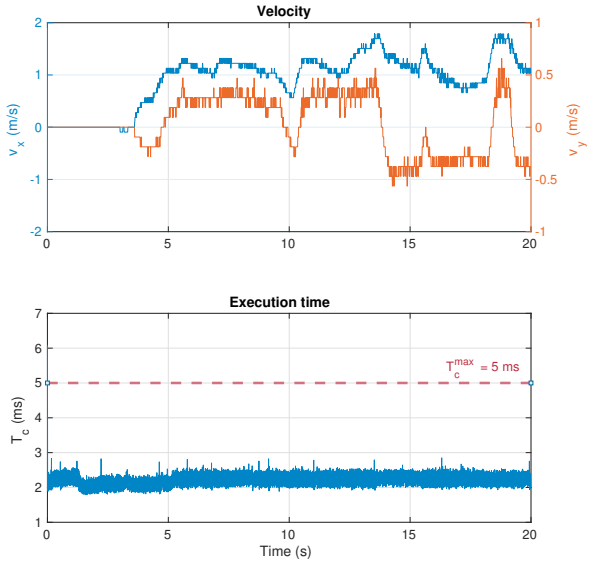

Fig. 5. RC car test: (top) measured velocities; (bottom) execution time

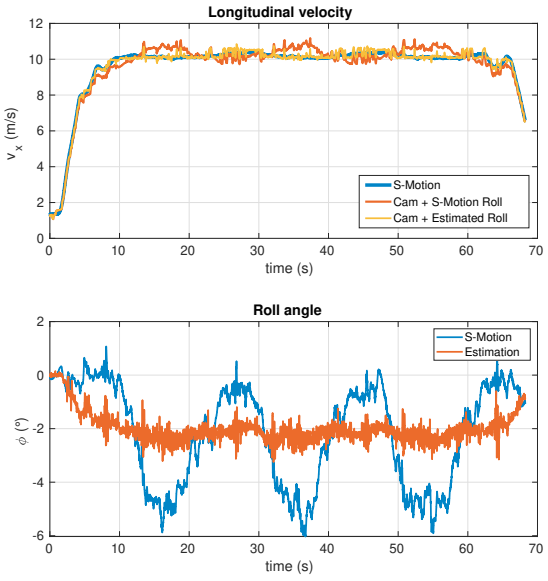

Fig. 6. Constant speed circle - ground truth and camera measurement using the roll angle provided by the S-Motion or the roll angle obtained by estimation

execution time, but the used platform, i.e. Intel NUC 12 with i7 1260p processor and Ubuntu 20.04 operating system, is not. Since it is not a real time system, other processes could be assigned higher priority thus delaying the computation of β. Instead, that is not an issue with the full-scale vehicle setup.

5. RESULTS

The main maneuver performed with the Alfa Romeo Giulia is a double lane change maneuver (DLC), according to the ISO standard 3888-2, conducted at 60 km/h. Two sets of tests were carried out, with the camera in location 1 first, and then moved to location 2. Before diving into those results, we present relevant insights on the effect of roll angle.

5.1 Effect of vehicle roll

When the camera is mounted on the vehicle side, the impact of roll angle on the height of the camera from the ground, $h(t)$, must be accounted for:

$$h(t) = h_0 + L \cdot sin(\phi(t)) \tag{3}$$

where $h(t)$ is the height of the camera, h_0 is the initial height, L is the lateral distance of the camera from the car longitudinal axis, $\phi(t)$ is the roll angle, which depends on the time t.

Roll angle information may be obtained from different sources:

- by approximating $\phi(t)$ as the integration of the roll rate, $\omega_x(t)$;
- from the Kistler S-Motion sensor, which provides an estimation of $\phi(t)$ (with an unknown estimation technique);
- by estimating $\phi(t)$ with a suitable model.

The resulting $\phi(t)$ from the first approach can drift in time due to integration procedure. The second approach is sufficiently reliable, but further tests showed that the roll angle provided by the S-Motion sensor includes the bank angle of the road, which the sensor cannot distinguish from roll angle. So, using such estimate (i.e., the sum of the vehicle roll angle and bank angle) in Eq. (3) and Eq. 2 would produce an incorrect result.

In light of the above, this work adopts the third approach. According to the mathematical vehicle model for road vehicle handling described in Guiggiani (2014), the steady-state $\phi(t)$ is linearly dependent on the vehicle lateral acceleration, a_y. The coefficient k_ϕ that relates ϕ to a_y may be easily obtained experimentally. Fig. 6 shows the results obtained over a constant radius maneuver (circle, 30 m radius) at constant speed, comparing the second (S-Motion) and third (linear dependence) approach. The ϕ angle provided by the S-Motion shows a periodic trend, confirming that the S-Motion estimate provides both the roll-angle of the vehicle and the bank angle of the road, which are respectively constant and periodic when performing a constant speed circle.

5.2 Kalman Filter integration

The camera measurements are noisy and present quantization issues. This is because the minimum measurable velocity corresponds to a single pixel displacement, that is a discrete quantity. Each pixel represents a fixed distance. The camera system is capable of observing a displacement only if, during the sampling time, the vehicle travels at least one pixel-distance. This problem, along with noisy signals, may be mitigated by means of Kalman filtering. We chose a kinematic model because accurate knowledge of the parameters of the dynamic model is not needed Chindamo et al. (2018). The model equations are:

$$\dot{v}_x = a_x + v_y \cdot r \tag{4}$$

$$\dot{v}_y = a_y - v_x \cdot r \tag{5}$$

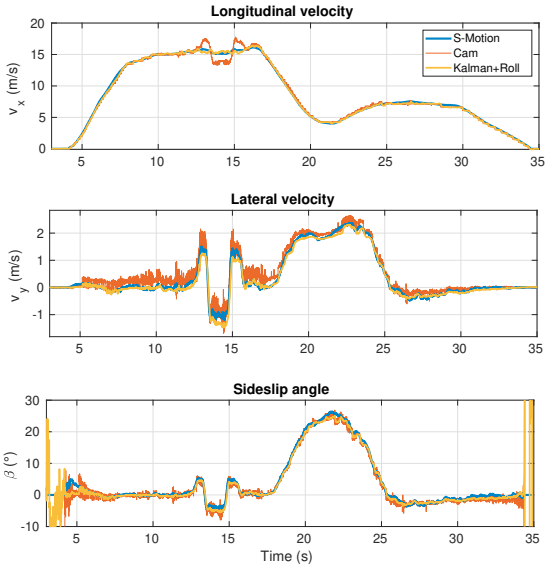

Fig. 7. DLC maneuver measurements with camera positioned in location 1

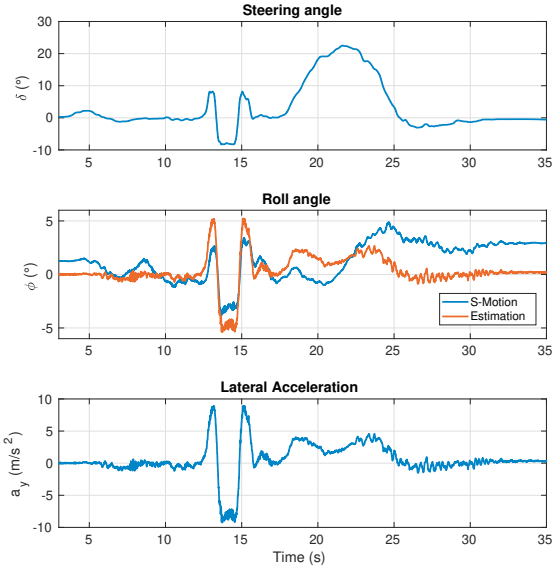

Fig. 8. DLC maneuver - Steering angle, roll angle and lateral acceleration when the camera positioned in location 1

where a_x and a_y are the vehicle longitudinal and lateral acceleration, v_x and v_y are the longitudinal and lateral components of the vehicle speed at the centre of mass, r is the yaw rate. The state of the system at a generic instant k is:

$$x(k) = [v_x(k)\ v_y(k)]^T \tag{6}$$

with input:

$$u(k) = [a_x(k)\ a_y(k)]^T \tag{7}$$

The model is discretised using Forward Euler, yielding:

$$A_d = \begin{bmatrix} 1 & r(k)dt \\ -r(k)dt & 1 \end{bmatrix} B_d = \begin{bmatrix} 1 \\ 1 \end{bmatrix} dt \tag{8}$$

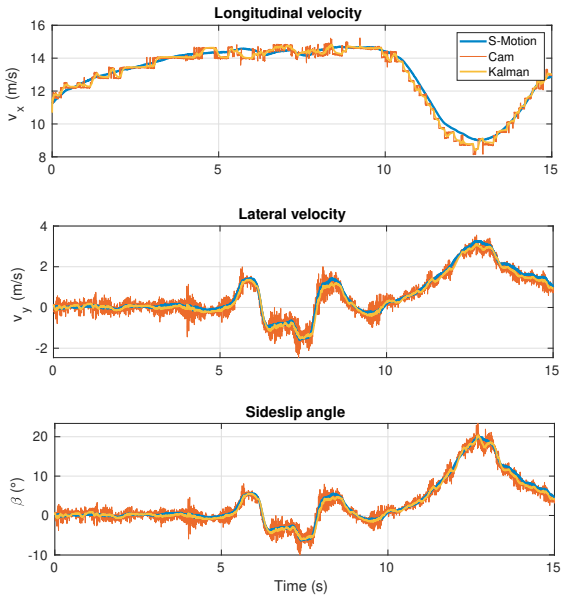

Fig. 9. DLC maneuver measurements with camera positioned in location 2

where dt is the sampling time. The measurement vector consists of the values of v_x and v_y calculated by the camera. The process covariance, $Q \in \mathbb{R}^2$, is based on the covariance of r and $a_{x,y}$ (obtained through the vehicle IMU), while the measurement covariance $R \in \mathbb{R}^2$ is based on the covariance of the camera:

$$Q = \begin{bmatrix} 3.6 \cdot 10^{-3} & 0 \\ 0 & 3.6 \cdot 10^{-3} \end{bmatrix} \tag{9}$$

$$R = \begin{bmatrix} 8.5 \cdot 10^{-2} & 0 \\ 0 & 8.5 \cdot 10^{-2} \end{bmatrix} \tag{10}$$

The results of the DLC with camera location 1 are depicted in Fig. 7. In the velocity plots, the roll angle has a remarkable impact on the camera measurement during the lane changes (from 12 s to 16 s). Interestingly, this effect does not appear in the sideslip angle plot, where the camera measurement is quite good. The reason is that $\beta = \arctan(v_y/v_x)$ and, looking back at Eq. 2, the height of the camera, h, cancels out. Another noteworthy observation is that the camera-measured lateral velocity plot shows an offset. This offset, not present at $v_y = 0$ m/s, is likely due to a camera angular offset along the x-axis.

Figure 8 depicts the steering angle of the vehicle, along with roll angle and lateral acceleration. In the roll angle plot notice that the ϕ provided by the S-Motion sensor is affected by bank angle, which is the reason of a nonzero signal from $t = 27$ s onwards. This is motivated by all other quantities indicating that the vehicle is driving straight (steering angle, lateral acceleration and lateral velocity), so that a zero roll angle would be expected. This further validates the herein used approach to estimate roll angle.

The results of the DLC with camera location 2 are depicted in Fig. 9, while steering angle and lateral acceleration are in Fig. 10. In this case the roll angle does not affect the camera measurements, but a Kalman filter approach has

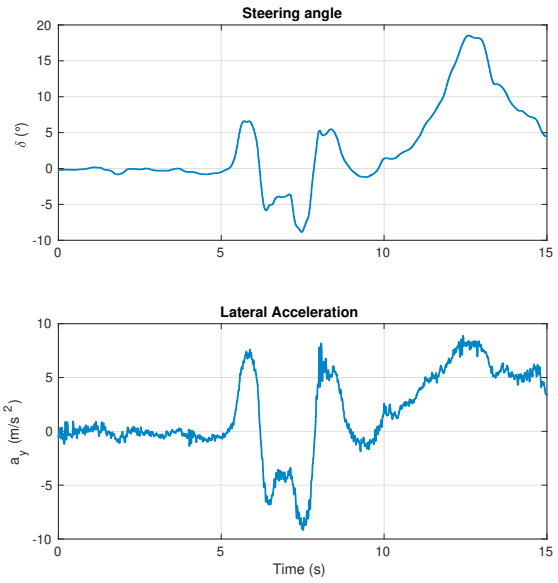

Fig. 10. DLC maneuver - Steering angle and lateral acceleration when the camera is in location 2

been used anyway to smooth the results. These results suggest that the accuracy of the longitudinal velocity and lateral velocity provided by the proposed solution strongly depends on the procedure to map the pixel displacement δ_x, δ_y, in which h is the only unknown variable. The sideslip angle measurement, instead, does not depend on the height of the camera.

6. CONCLUSION

In this work we proposed a novel solution to provide a consistent and accurate measure of sideslip angle, unlike typical model based or data driven estimation methods. The new approach exploits computer vision techniques, and it has been tested on both a RC vehicle and on a full-scale vehicle to validate the solution against a cutting edge sideslip angle optical sensor (cost around 25000 €). We also showed that the placement of the camera is an important practical aspect that plays a key role in the accuracy of the estimator. Installing the camera on the side of the vehicle (e.g. under the side mirrors) makes the estimator more sensitive to vehicle roll angle, when compared to the rear-center mounting. To cancel the impact of this disturbance, we applied a pragmatic roll estimator. The experimental validation demonstrated that the proposed method offers a level of accuracy similar to Kistler's optical sensor, with a very significant cost reduction.

7. ACKNOWLEDGEMENTS

This work was supported in part by the Italian Ministry of Foreign Affairs and International Cooperation, grant number PGR02074, US23GR13.

REFERENCES

Beaver, J. (2018). *The Physics and Art of Photography, Volume 1: Geometry and the nature of light*. Morgan & Claypool Publishers.

Birem, M., Kleihorst, R., and El-Ghouti, N. (2018). Visual odometry based on the fourier transform using a monocular ground-facing camera. 14(3), 637–646.

Botha, T.R. and Els, P.S. (2014). Tire longitudinal slip-ratio measurement using a camera. In *Volume 3: 16th Int. Conf. on Advanced Vehicle Technologies*.

Botha, T.R. and Els, P.S. (2015). Digital image correlation techniques for measuring tyre-road interface parameters: Part 1 – side-slip angle measurement on rough terrain. 61, 87–100.

Chindamo, D., Lenzo, B., and Gadola, M. (2018). On the vehicle sideslip angle estimation: A literature review of methods, models, and innovations. 8(3), 355.

De Martino, M., Farroni, F., Pasquino, N., Sakhnevych, A., and Timpone, F. (2017). Real-time estimation of the vehicle sideslip angle through regression based on principal component analysis and neural networks. In *IEEE International Systems Engineering Symposium*, 1–6.

Guiggiani, M. (2014). *The Science of Vehicle Dynamics*. Springer.

Hsu, Y.H.J., Laws, S.M., and Gerdes, J.C. (2009). Estimation of tire slip angle and friction limits using steering torque. *IEEE Transactions on Control Systems Technology*, 18(4), 896–907.

Johnson, D.K., Botha, T.R., and Els, P.S. (2019). Real-time side-slip angle measurements using digital image correlation. 81, 35–42.

Katriniok, A. and Abel, D. (2016). Adaptive ekf-based vehicle state estimation with online assessment of local observability. *IEEE Transactions on Control Systems Technology*, 24(4), 1368–1381.

Kazik, T. and Goktogan, A.H. (2011). Visual odometry based on the fourier-mellin transform for a rover using a monocular ground-facing camera. In *2011 IEEE International Conference on Mechatronics*, 469–474.

Kuyt, C. and Como, M. (2018). Mixed kinematics and camera based vehicle dynamic sideslip estimation for an RC scaled model. IEEE.

Lenzo, B. (2022). Torque vectoring control for enhancing vehicle safety and energy efficiency. In *Vehicle Dynamics: Fundamentals and Ultimate Trends*, 193–233. Springer.

Mosconi, L., Farroni, F., Sakhnevych, A., Timpone, F., and Gerbino, F. (2022). Adaptive vehicle dynamics state estimator for onboard automotive applications and performance analysis. *Vehicle System Dynamics*, 61.

Serena, L., Lenzo, B., Bruschetta, M., and De Castro, R. (2023). Computer vision approaches for vehicle sideslip angle estimation. In *IEEE International Workshop on Metrology for Automotive*.

Viehweger, M., Vaseur, C., van Aalst, S., Acosta, M., Regolin, E., Alatorre, A., Desmet, W., Naets, F., Ivanov, V., Ferrara, A., et al. (2021). Vehicle state and tyre force estimation: demonstrations and guidelines. *Vehicle system dynamics*, 59(5), 675–702.

Xia, X., Hashemi, E., Xiong, L., and Khajepour, A. (2023). Autonomous vehicle kinematics and dynamics synthesis for sideslip angle estimation based on consensus kalman filter. *IEEE Transactions on Control Systems Technology*, 31(1), 179–192.